chemosensors

MDPI

Article

Electrochemical Mercury Biosensor Based on Electrocatalytic Properties of Prussian Blue and Inhibition of Catalase

Povilas Virbickas, Narvydas Dėnas and Aušra Valiūnienė *

Faculty of Chemistry and Geosciences, Vilnius University, Naugarduko 24, LT-03225 Vilnius, Lithuania; povilas.virbickas@chgf.vu.lt (P.V.); narvydas.denas@chgf.stud.vu.lt (N.D.)
* Correspondence: ausra.valiuniene@chf.vu.lt

Abstract: This paper presents a detailed study of a novel type of electrochemical mercury ion (Hg^{2+}) biosensor developed by combining Prussian blue (PB) and catalase (Cat). The simultaneous PB-catalyzed reduction of hydrogen peroxide and the inhibition of catalase by Hg^{2+} ions were used as the working principle of the biosensor. The biosensor described in this research was capable of detecting Hg^{2+} ions at relatively low potentials (+0.2 V vs. Ag | AgCl, KCl_{sat}) using chronoamperometry and a fast Fourier transform electrochemical impedance spectroscopy (FFT-EIS). Linear ranges of 0.07 mM–3 mM and 0.13 mM–0.80 mM of Hg^{2+} ions were obtained using amperometric and impedimetric techniques, respectively. In the course of this work, an amperometric study of the Hg^{2+} ion biosensor was also carried out on a real sample (tap water containing Hg^{2+} ions).

Keywords: mercury ion; Prussian blue; catalase; biosensor; electrochemical impedance spectroscopy; chronoamperometry

Citation: Virbickas, P.; Dėnas, N.; Valiūnienė, A. Electrochemical Mercury Biosensor Based on Electrocatalytic Properties of Prussian Blue and Inhibition of Catalase. *Chemosensors* **2023**, *11*, 311. https://doi.org/10.3390/chemosensors11050311

Academic Editor: Manel del Valle

Received: 6 April 2023
Revised: 5 May 2023
Accepted: 17 May 2023
Published: 22 May 2023

1. Introduction

Mercury is a heavy metal that can exist in different forms: an inorganic form, which consists of metallic mercury (Hg^0) and mercury ions (Hg_2^{2+} and Hg^{2+}), and an organic form, which is formed when mercury is attached to structures containing carbon atoms (methyl, ethyl, phenyl or similar groups) [1]. Mercury and its derivatives are highly toxic to humans and other living species. In the human body, Hg^{2+} is retained in brain tissue, where mercury can be present for many years. Many intracellular processes in the brain can be affected, including DNA, RNA and protein synthesis, microtubule polymerization, cell division and cell migration [2–6]. In many cases, the toxic effect of Hg^{2+} is related to enzyme inhibition, since Hg^{2+} ions tend to interact with the thiol group (-SH) of proteins and other biologically active compounds [7]. In the case of catalase, the inhibition caused by Hg^{2+} ions is based on van der Waals and the electrostatic interactions between Hg^{2+} and catalase [8]. These interactions between catalase and Hg^{2+} lead to changes in the conformation of catalase, which is believed to reduce the activity of catalase [8].

Mercury can be released into the environment naturally through volcanic activity and rock weathering [9,10]. However, human industrial activities, e.g., metal mining and the chlor-alkali industry [9,11,12], are also important sources of mercury contamination of the environment—due to anthropogenic activities, the global atmospheric Hg deposition rate has increased about three times compared to that of pre-industrial times [13]. Particularly high levels of mercury contamination are found in the soil of industrialized areas, where the concentration of mercury can reach 9000 ppm [14]; in the water near plants or mined areas, the concentration of mercury can reach more than 7 ppb [15]. Taking into account that concentrations of mercury can vary drastically depending on the sampling location as well as on the type of sample analyzed [10–15], the development of analytical methods suitable for analyzing different ranges of mercury concentrations is of great importance.

Mercury can be detected by various analytical methods such as cold vapor atomic absorption spectroscopy (CVAAS) [16–18], cold vapor atomic fluorescence spectroscopy

(CVAFS) [19,20], inductively coupled plasma mass spectrometry (ICP-MS) [19,21] and graphite furnace atomic absorption spectrometry (GFAAS) [22,23]. These methods are sensitive and have high reproducibility. However, the use of these methods requires large amounts of chemical reagents, expensive equipment and analysis and are not time efficient [24,25]. Nevertheless, concentrations of mercury can also be measured using biosensors, which are characterized by their inherent simplicity, rapid analysis and small size, as well as ease of operation [26]. There have been many scientific investigations [27–35] which have aimed to determine Hg^{2+} ion concentrations in solutions using various biosensors based on DNA, enzymes, such as catalase, glucose oxidase and urease, and different electrochemical measurement approaches [27–35]. However, earlier-developed Hg^{2+} ion biosensors often faced problems that hindered the development of an efficient and applicable biosensor for the analysis of real samples, e.g., narrow linear range [27,28,30,32,35], disposability [30] and a requirement to use complex and expensive systems [29,33].

In this work, an electrochemicalHg^{2+} ion biosensor was developed by modifying the surface of a fluorine-doped tin oxide-coated glass electrode (glass | FTO) with a layer of Prussian blue (PB), and then immobilizing the enzyme catalase (Cat). To the best of our knowledge, a Hg^{2+} ion biosensor developed by combining PB and catalase has never been reported. This biosensor, based on the developed electrode (glass | FTO | PB | Cat), was able to measure the concentration of Hg^{2+} ions in aqueous solutions using amperometric and impedimetric techniques. The working principle of this biosensor is based on the simultaneous PB-catalyzed reduction of hydrogen peroxide and catalase inhibition by the Hg^{2+} ions.

2. Materials and Methods

2.1. Materials

K_2HPO_4 (purity $\geq$ 99%, CAS No. 7758-11-4), H_3PO_4 (purity 85%, CAS No. 7664-38-2), $K_3[Fe(CN)_6]$ (purity $\geq$ 99%, CAS No. 13746-66-2), $FeCl_3 \cdot 6H_2O$ (purity $\geq$ 98%, CAS No. 10025-77-1), KCl (purity $\geq$ 99.5%, CAS No. 7447-40-7), acetone (purity $\geq$ 99.9%, CAS No. [67-64-1]), HCl (37%, CAS No. 7647-01-0) and catalase (purity $\geq$ 11 700 U/mg material, CAS No. 9001-05-2) were acquired from ROTH (Karlsruhe, Germany). A 2% Mikro-90 solution and glutaraldehyde 25% (grade II, CAS No. 111-30-8) were acquired from Sigma Aldrich (Munich, Germany). Ultrapure water (R $\geq$ 18 MΩ $\times$ cm) supplied by a Milli Q-plus-Millipore system (Burlington, NJ, USA) was used to prepare all the solutions. A phosphate buffer solution (PBS) (pH 7) was prepared by dissolving K_2HPO_4 (10 mmol/L) and adjusting the pH value using H_3PO_4 solution to pH 7.

2.2. Equipment

Chronoamperometric and cyclic voltammetry-based measurements were performed using a µAUTOLAB potentiostat/galvanostat from ECO-Chemie (Utrecht, The Netherlands).

pH measurements were performed using a pH meter HI83141 with an HI1230B electrode from Hanna Instruments (Bedfordview, Republic of South Africa).

Fast Fourier transform electrochemical impedance spectroscopy (FFT-EIS) measurements were performed with a FFT impedance spectrometer EIS-128/16 constructed by Prof. G. Popkirov (University of Kiel, Germany) [36]. In FFT-EIS, a 16-bit digital-to-analog converter can create a perturbation signal as a sum of up to 80 frequencies and apply it to the sample. This technique allows for a drastic reduction in the required measurement time. For example, a full impedance spectrum from 1 Hz to 10 kHz can be obtained in 2 s.

2.3. Fabrication of the Glass | FTO | PB | Cat Electrode

Prior to biosensor fabrication, the glass | FTO plate was cleaned [37] using sonification in (1) 2% Micro-90 solution, (2) acetone and (3) deionized water for 16 min during each step (1, 2 and 3). During the PB-layer deposition, the potential of the previously cleaned glass | FTO plate was scanned from 0.4 V to 0.8 V vs. Ag | AgCl, KCl_{sat} (scan rate 40 mV s^{-1}) in the solution, containing 1 mmol/L $K_3[Fe(CN)_6]$, 1 mM $FeCl_3 \cdot 6H_2O$ and 0.1 M HCl [38]. A total of 40 potential cycles were applied. To stabilize the PB layer [39] deposited on the

glass | FTO | PB electrode, potential scanning in a range from 0.45 V to 0 V vs. Ag | AgCl, $KCl_{sat,}$ at a scan rate of 40 mV s^{-1}, was applied in a solution containing 0.1 M KCl and 0.1 M HCl. A total of 20 potential cycles were applied. To immobilize catalase on the glass | FTO | PB electrode, 25 µL of 5 mg/mL catalase solution was distributed on 1 cm^2 geometric area of the PB surface and left to dry at ambient conditions. Then, the fabricated glass | FTO | PB | Cat electrode was held over a 25% glutaraldehyde aqueous solution for 15 min for cross-linking the catalase enzyme to immobilize it [38,39]. After catalase immobilization, the glass | FTO | PB | Cat electrode was rinsed with deionized water to remove any residual glutaraldehyde. Optical microscope images of the glass | FTO | PB plate recorded before and after the immobilization of the catalase are shown in Figure 1. It was found that before catalase immobilization the PB coating on the glass | FTO plate was rather smooth and blue in color (Figure 1A), while after catalase immobilization (Figure 1B), white spots of catalase enzymes were observed on the glass | FTO | PB plate.

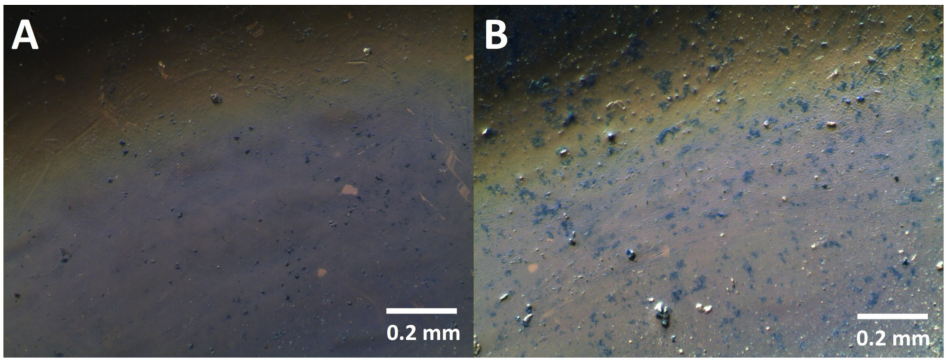

Figure 1. Optical microscope images (zoomed in 40 times) of the PB-coated glass | FTO plate (**A**) before immobilization of catalase with glutaraldehyde and (**B**) after immobilization of catalase with glutaraldehyde.

2.4. Electrochemical Measurements

All the electrochemical measurements were carried out at room temperature (25 ± 1 °C) and at standard pressure (760 ± 25 mmHg). The experiments were performed using a three-electrode system consisting of the glass | FTO | PB or the glass | FTO | PB | Cat working electrode, a platinum wire as a counter electrode and a Ag | AgCl, KCl_{sat} electrode as a reference electrode. To characterize the amperometric and impedimetric response of the glass | FTO | PB | Cat electrode to the Hg^{2+} ions, at least 6 electrodes were used in this research.

During the amperometric measurements, the solution in the electrochemical cell was stirred with a magnetic stirrer (~2 revolutions per second (RPS)) throughout the experiment. An amount of either 0.088 M H_2O_2 or 0.1 M $HgCl_2$ (from 0.011 mM to 3 mM) solution was added to the PBS only after a constant current was reached, which was attributed to the background current of the electrochemical system.

The FFT-electrochemical impedance spectra were recorded at the potentiostatic mode (by applying 0.2 V vs. Ag | AgCl, KCl_{sat}), and the range of alternating current frequencies varied from 2 Hz to 10.5 kHz, allowing for a single spectra to be recorded within 1 s. The data analysis software "Zview" was used to analyze the experimental data according to the model containing the elements of selected equivalent circuit. In these FFT-EIS studies, after the addition of H_2O_2 (0.88 M) or $HgCl_2$ (0.1 M) stock solution to the PBS, the solution was further stirred (2 RPS) for 1 min and then allowed to settle for 0.5 min to avoid any unnecessary relaxation effects that can be a source of distortion in the FFT-EIS measurement data.

3. Results and Discussion

3.1. Amperometric Study of the Hg^{2+} Ion Biosensor Based on the Glass | FTO | PB | Cat Electrode

In order to develop an electrochemical-catalase inhibition-based biosensor for a Hg^{2+} ion, it is necessary to relate the inhibition of catalase to an electrochemical signal, e.g., to measure the reduction current of hydrogen peroxide, which is a substrate of the enzyme catalase. For

this purpose, Prussian blue (PB) could be used in the composition of the Hg^{2+} ion biosensor because PB is a well-known electrocatalyst of H_2O_2 reduction (Equation (1)) [40].

$$H_2O_2 + 2H^+ + 2e^- \overset{PB}{\rightarrow} 2H_2O \quad (1)$$

$$2H_2O_2 \overset{Cat}{\rightarrow} H_2O + O_2 \quad (2)$$

Considering that the enzyme catalase disproportionates H_2O_2 to oxygen and water (Equation (2)) [41], and PB catalyzes the electrochemical reduction of H_2O_2 (Equation (1)), in this research it was decided to develop a Hg^{2+} ion biosensor by immobilizing catalase (Cat) on the glass | FTO | PB electrode. As can be expected, the electrochemical response of such a Hg^{2+} ion biosensor (glass | FTO | PB | Cat) should be dependent on the H_2O_2 disproportionation reaction (Equation (2)), because the amount of H_2O_2 reaching the PB layer will be decreased due to the disproportionation of H_2O_2 by catalase, causing a relevant decrease in the cathodic current of the H_2O_2 reduction at the glass | FTO | PB electrode. On the other hand, the addition of Hg^{2+} ions to the H_2O_2-containing PBS may cause the inhibition of catalase, resulting in a decreased rate of catalytic H_2O_2 disproportionation and an increased rate of the electrochemical-PB-catalyzed H_2O_2 reduction. Therefore, the increase in the rate of the H_2O_2 reduction on the PB layer can be used for the electrochemical detection of Hg^{2+} ions. Specifically, both amperometric and impedimetric techniques can be used to detect Hg^{2+} ions using the glass | FTO | PB | Cat electrode developed in this research.

Previously reported [30] catalase inhibition-based Hg^{2+} ion biosensors required a three-step approach for Hg^{2+} ion sensing, which included: (i) measuring the H_2O_2 reduction current with a Hg^{2+}-unaffected biosensor, (ii) incubating the biosensor in a Hg^{2+} ion-containing solution and (iii) measuring the H_2O_2 reduction current after incubating the biosensor in a Hg^{2+} ion-containing solution. In this work, it was decided to develop a Hg^{2+} ion biosensor capable of detecting Hg^{2+} ions without incubating the biosensor in a solution containing Hg^{2+} ions. To achieve this, a Hg^{2+} ion biosensor based on catalase inhibition should be able to operate in a solution containing both H_2O_2 and Hg^{2+} ions. Therefore, it is important to select the appropriate potential at which the electrochemical reduction of H_2O_2 occurs without redox reactions of Hg^{2+} ions. It is known from previous studies [38,42,43] that PB-catalyzed H_2O_2 reduction occurs only at potentials lower than 0.15 V–0.27 V vs. Ag | AgCl, KCl_{sat}, depending on the electrode material and/or the composition of the electrolyte. In this study, the glass | FTO | PB electrode was electrochemically tested by adding Hg^{2+} and H_2O_2 to the PBS at potentials of +0.1 V and +0.2 V (vs. Ag | AgCl, KCl_{sat}) (Figure 2). As can be seen in Figure 2, when a potential of +0.2 V was applied to the glass | FTO | PB electrode, the addition of Hg^{2+} ions to the PBS did not cause any changes to the current registered on the electrode; however, after the addition of H_2O_2 to the solution, the reduction current started to increase sharply (Figure 2, black curve).

This finding indicates that a potential of +0.2 V vs. Ag | AgCl, KCl_{sat} is suitable for measuring a H_2O_2 reduction reaction (Equation (1)), even with the presence of Hg^{2+} ions in the solution. Moreover, such a low potential for the working electrode (+0.2 V (vs. Ag | AgCl, KCl_{sat})) helps to avoid the interfering oxidation reactions of the other electrochemically active substances which might be present in the sample, e.g., alkylphenols and sulfite ions [44,45]. Nevertheless, in this study it was decided to test the glass | FTO | PB electrode using chonoamperometry at an even lower potential of + 0.1 V vs. Ag | AgCl, KCl_{sat} (Figure 2, gray curve). However, it was found that when a potential of +0.1 V vs. Ag | AgCl, KCl_{sat} was applied to the glass | FTO | PB electrode, the cathodic current began to increase rapidly after the addition of Hg^{2+} ions to the PBS, due to the reduction of Hg^{2+} ions (Figure 2, gray curve). Therefore, when +0.1 V is applied to the glass | FTO | PB electrode, an increase in the cathodic current caused by the addition of H_2O_2 would be inseparable from the Hg^{2+} ion reduction current. Therefore, a potential value of +0.2 V was used in further investigations of the Hg^{2+} ion biosensor based on the glass | FTO | PB | Cat electrode.

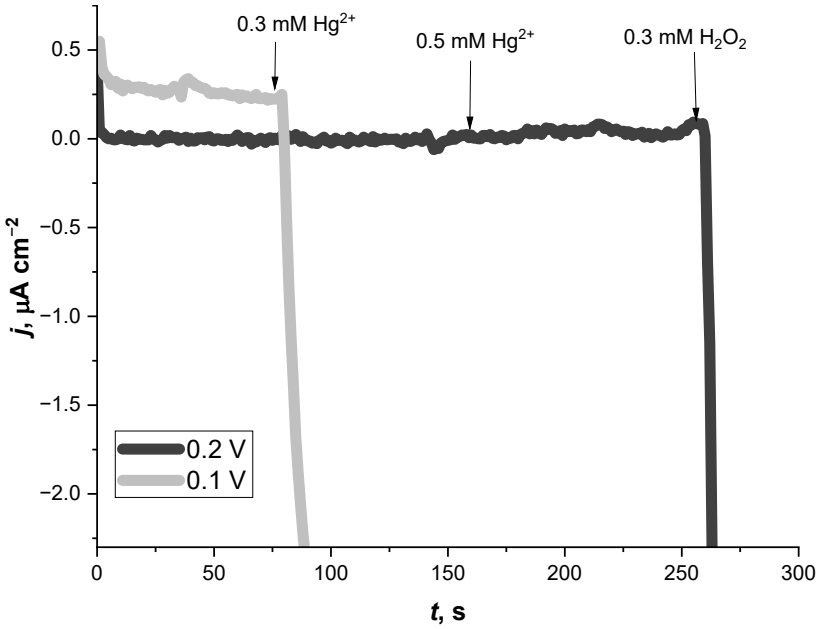

Figure 2. Chronoamperograms of the glass | FTO | PB electrode in the PBS measured at +0.2 V (black curve) and at +0.1 V (gray curve) vs. the Ag | AgCl, KCl_{sat} reference electrode.

An amperometric study of the glass | FTO | PB | Cat electrode in the PBS (Figure 3A) showed that the initial addition of 0.3 mM of H_2O_2 resulted in only a negligible (-0.7 µA cm^{-2}) cathodic current. The small value (-0.7 µA cm^{-2}) of the H_2O_2 reduction current indicates that the catalase efficiently disproportionated H_2O_2 into water and oxygen (Equation (2)); thus, most of the H_2O_2 from the solution was unable to penetrate the catalase coating of the glass | FTO | PB | Cat electrode and reach the PB layer. Meanwhile, the addition of Hg^{2+} ions to the PBS resulted in a significant increase in the cathodic current of the glass | FTO | PB | Cat electrode. Particularly, the cathodic current increased by approx. 45 µA cm^{-2} after adding 3 mM of Hg^{2+} to the PBS (Figure 3B). Therefore, after the addition of Hg^{2+} ions to the H_2O_2-containing PBS, more H_2O_2 molecules were able to penetrate through the catalase coating and be electrochemically reduced on the PB layer (Equation (1)). This Hg^{2+}-caused increase in the cathodic current appears to be linearly dependent ($R^2 = 0.994$) on the Hg^{2+} concentration in the range of 0.07 mM to 3 mM of Hg^{2+} (Figure 3B), with a sensitivity of 15 µA cm^{-2} mM^{-1}. For the sake of comparison, the linear concentration ranges of other electrochemical-enzyme inhibition-based Hg^{2+} biosensors ranged from 5×10^{-4} µM–27 µM to 5×10^{-7}–0.25 mM (Table 1). Therefore, the glass | FTO | PB | Cat electrode-basedHg^{2+} ion biosensor seems to be suitable for analyzing samples containing higher concentration of Hg^{2+}, such as contaminated water and extracts made from soil or sediments [9,11–14].

3.2. Stability of the Hg^{2+} Ion Biosensor Based on the Glass | FTO | PB | Cat Electrode

In order to evaluate the stability of the glass | FTO | PB | Cat biosensor response to Hg^{2+} ions over time, the sensitivity of the Hg^{2+} ion biosensor was tested continuously for 70 days by examining the chronoamperometric responses of the FTO | PB | Cat electrode in PBS containing different concentrations of Hg^{2+} ions. A single glass | FTO | PB | Cat electrode was tested seven times: during the day of its preparation and after 14, 21, 28, 35, 56 and 70 days after its preparation, respectively. Between measurements, the glass | FTO | PB | Cat electrode was stored in a refrigerator ($t = 4 \pm 1$ °C) under dry conditions. From the obtained linear dependencies between the cathodic current and the concentration of Hg^{2+} ions, it was found that the sensitivity of the biosensor decreased with time (Table 2), indicating some changes in the stability of the biosensor over time.

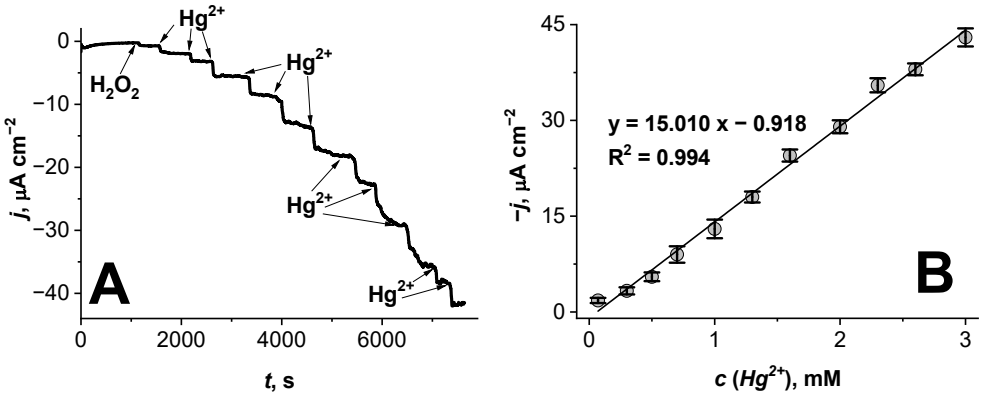

Figure 3. (**A**) An amperometric investigation of the biosensor based on the glass | FTO | PB | Cat electrode at 0.2 V potential vs. Ag | AgCl, KCl_{sat} in PBS (pH 7), with the addition of 0.3 mM H_2O_2 and varying amounts of Hg^{2+} ions. Symbols "H_2O_2" and "Hg^{2+}" indicate the time of adding these compounds to PBS. *t*—time (s), *i*—current density (μA cm^{-2}). (**B**) The linear dependence of the Hg^{2+}-induced increase in the cathodic current on the concentration of Hg^{2+} ions (*c* (Hg^{2+})) in PBS.

Table 1. Linear range, stability, sensitivity and storage conditions of the electrochemical-enzyme inhibition-based Hg^{2+} ion biosensors.

Biosensor	Linear Range, M	Sensitivity	Stability	Storing Conditions	Reference
Pt/PPy-GOx	2.5×10^{-8}–5×10^{-6}	7.46 mV mM^{-1}	>90% initial sensitivity after 8 consecutive measurements	In PBS	[46]
(CS/GLM)8-GCE	5×10^{-7}–5×10^{-6}	-	85% initial sensitivity after 72 h	At room temperature under dry conditions	[47]
Ultrathin Ppy | GOx	4.8×10^{-7}–3.3×10^{-6}	4.0 μA cm^{-2} μM^{-1}	40% initial sensitivity after 3 weeks	-	[28]
GCE | Cat	5×10^{-11}–5×10^{-10}	0.44 inhibition% nM^{-1}	40% initial sensitivity after 3 weeks (3 measurements)	-	[30]
Glass | FTO | PB | GOx	2.7×10^{-5}–2.5×10^{-4}	0.164 inhibition% μM^{-1}	72% initial sensitivity after one measurement	-	[48]
GCE/MWCNTs-RuO_2/GOx/Nafion®®	5×10^{-6}–8×10^{-5}	5 μA^{-1} mM^{-1}	-	-	[49]
Pt | PPD | Gox	5×10^{-6}–1.8×10^{-4}	0.067 μA^{-1} μM^{-1}	60% initial sensitivity after 24 h	In PBS	[31]
Glass | FTO | PB | Cat	7×10^{-5}–3×10^{-3}	15 μA cm^{-2} mM^{-1}	90% initial sensitivity after 2 weeks	In a refrigerator (t = 4 ± 1 °C) under dry conditions	This study

Table 2. Variation of the biosensor based on the glass | FTO | PB | Cat electrode sensitivity to Hg^{2+} ions over time.

Days after Production of the Biosensor	Sensitivity, μA cm^{-2} mM^{-1}	R^2
Freshly prepared	15.01	0.992
1	13.78	0.998
14	13.33	0.993
21	10.16	0.991
28	10.09	0.989
35	9.06	0.991
56	8.02	0.998
70	4.59	0.990

As can be seen from the data in Table 2, the sensitivity of the Hg^{2+} biosensor based on the glass | FTO | PB | Cat electrode decreased only about 10% during the first 2 weeks and did not decrease much within the 28-day period, remaining at 66.7% of the initial sensitivity. After 10 weeks, the biosensor lost about 65% of its initial sensitivity, but still showed a sensitivity of 4.59 μA cm^{-2} mM^{-1}. Other similar electrochemical-enzyme

inhibition-based Hg^{2+} ion biosensors showed a fluctuating loss of sensitivity (Table 1). For example, depending on the composition of the enzyme inhibition-based Hg^{2+} ion biosensor, a sensitivity loss of 25% after the first calibration curve, a loss of 60% after 3 weeks or a loss of 40% after 24 h was observed (Table 1).

In summary, it can be concluded that the Hg^{2+} ion biosensor constructed in this research has some advantages compared to other biosensors for mercury detection [28,30,32,33]. Its amperometric responses showed good linear dependencies for the construction of calibration curves ($R^2 \approx 0.99$), which are well suited for the calculation of the sensitivity, which was found to be comparatively high (15.01 μA cm^{-2} mM^{-1}) for the wide concentration range of the Hg^{2+} ions (0.07 mM to 3 mM). Furthermore, the decrease in the sensitivity of our developed Hg^{2+} ion biosensor was rather small during the 2-week period, indicating that the biosensor does not need to be prepared before each measurement, but can be prepared in advance for later use.

3.3. Investigation of the Hg^{2+} Biosensor in Tap Water

In comparison to the chronoamperometric investigation of the Hg^{2+} ion biosensor in PBS (Figure 3A), the detection of Hg^{2+} ions in tap water allowed us to register some increase in the cathodic current after the addition of very low concentrations of Hg^{2+} ions (from 11 μM to 300 μM); however, the amperometric responses in tap water at such low Hg^{2+} concentrations were not linearly proportional to the Hg^{2+} concentration. Meanwhile, increasing the Hg^{2+} concentration in tap water from 0.3 mM to 1.5 mM resulted in a linear dependence between the cathodic current and the concentration of Hg^{2+} ions (Figure 4A,B). The sensitivity of the Hg^{2+} ion biosensor in tap water (Figure 4B) was slightly lower (13.29 μA cm^{-2} mM^{-1}) than in PBS (Figure 3B) (15.01 μA cm^{-2} mM^{-1}). These results are due to the matrix effect, indicating that the standard addition method has to be used for real samples analysis. Considering that Hg^{2+} concentration measurement in PBS has a higher sensitivity, we can conclude that PBS is more suitable for measuring Hg^{2+} ion concentration than tap water, but our developed Hg^{2+} biosensor can also be used for the preliminary analysis of mercury ions in tap water.

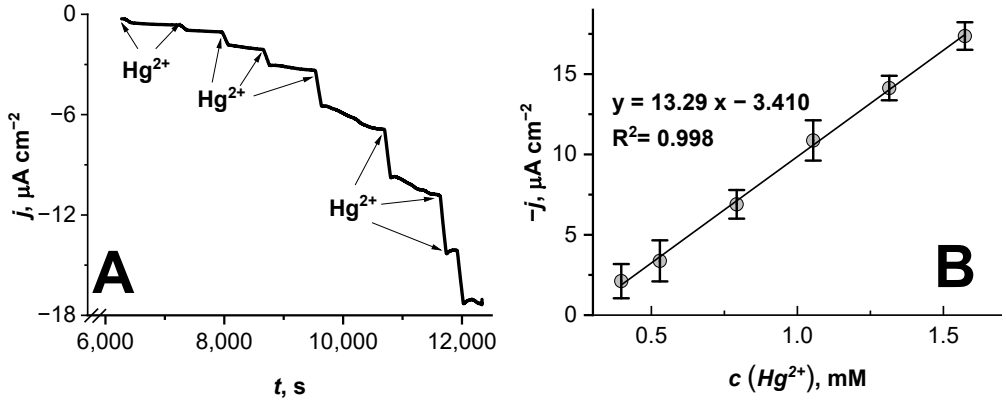

Figure 4. (**A**) The amperometric investigation of the Hg^{2+} biosensor based on the glass | FTO | PB | Cat electrode at 0.2 V potential vs. Ag | AgCl, KCl_{sat} in tap water, with the addition of 0.3 mM H_2O_2 and varying amounts of Hg^{2+} ions. The symbol "Hg^{2+}" indicates the time of addition of Hg^{2+} to tap water. *t*—time (s), *i*—current density (μA cm^{-2}). (**B**) The linear dependence of the Hg^{2+}-induced increase in the cathodic current on the concentration of Hg^{2+} ions (*c* (Hg^{2+})) in tap water.

3.4. Investigation of the Hg^{2+} Biosensor Using Fast Fourier Transform Electrochemical Impedance Spectroscopy

To determine the kinetic parameters of the system and to design an impedimetric Hg^{2+} ion biosensor based on the glass | FTO | PB | Cat electrode, fast Fourier transform electrochemical impedance spectroscopy (FFT-EIS) measurements were performed at a potential of 0.2 V vs. Ag | AgCl, KCl_{sat}: (i) in PBS (pH 7), (ii) with the addition of 0.3 mM

H_2O_2 to the PBS and (iii) with the addition of varying amounts of Hg^{2+} ions (from 0.13 mM to 0.8 mM) to the PBS (Figure 5).

The FFT-EIS spectra in the Nyquist plot (Figure 5) showed that the addition of H_2O_2 to the PBS did not significantly affect the shape of the electrochemical impedance spectrum (Figure 5, curves 1 and 2), which could be explained by the rather effective disproportionation of H_2O_2 by catalase (Equation (2)). Meanwhile, when Hg^{2+} ions were added to the PBS, the diameter of the uncomplete semicircle decreased as a function of the concentration of Hg^{2+} ions added (Figure 5, curves 3–7). This is an indication that Hg^{2+} ions facilitate a charge transfer at the electrode/PBS interface. Similar to the amperometric investigation of the Hg^{2+} biosensor in Hg^{2+} ions containing PBS (Figure 3), the enhancing effect of Hg^{2+} ions on the charge transfer can be explained by the inhibition of catalase with Hg^{2+} ions: since catalase is inhibited with Hg^{2+} ions, more H_2O_2 molecules can penetrate through the catalase layer and be electrochemically reduced on the PB layer (Equation (1)).

FFT-EIS data (Figure 5) for the Hg^{2+} biosensor constructed in this study were analyzed using the Randles circuit model (Figure 5, inset), which consists of the solution resistance (R_s), constant phase element (*CPE*) and charge transfer resistance (R_{ct}). The electrochemical parameters obtained by analyzing the FFT-EIS data (Figure 5) are listed in Table 3.

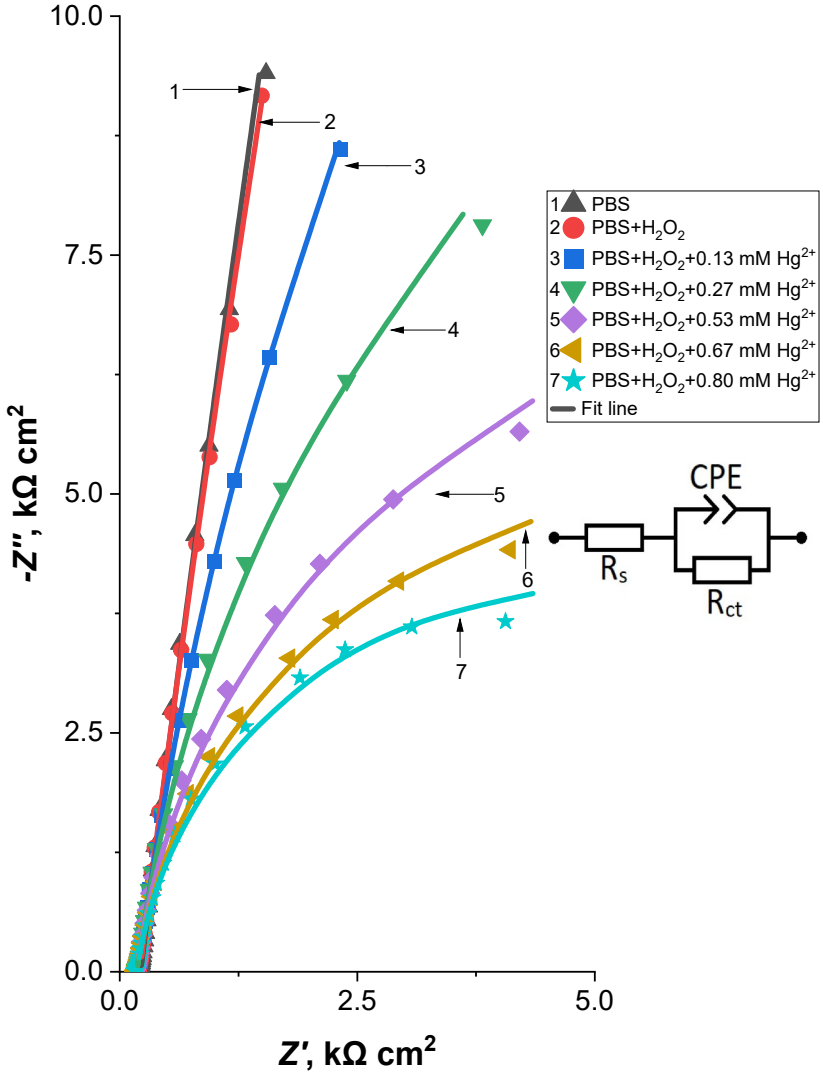

Figure 5. FFT-EIS spectra of the Hg^{2+} ion biosensor based on the glass | FTO | PB | Cat electrode at 0.2 V potential vs. Ag | AgCl, KCl_{sat} in PBS (pH 7), with the addition of 0.3 mM H_2O_2 and varying amounts of Hg^{2+} ions (from 0.13 mM to 0.8 mM).

Table 3. Electrochemical parameters obtained by fitting the FFT-EIS data (Figure 5) to the equivalent circuit model (Figure 5, inset).

Solution Composition	R_s, Ω cm^2	*CPE*, μF cm^{-2}	*n* (CPE)	R_{ct}, kΩ cm^2
PBS (pH 7)	219.2	9.45	0.92	960
PBS + 0.3 μM H_2O_2	209.6	9.64	0.92	576
PBS + 0.3 μM H_2O_2 + 0.13 mM $HgCl_2$	195.8	9.92	0.92	80.3
PBS + 0.3 μM H_2O_2 + 0.27 mM $HgCl_2$	181.5	9.70	0.92	31
PBS + 0.3 μM H_2O_2 + 0.53 mM $HgCl_2$	178.2	10.03	0.92	15.7
PBS + 0.3 μM H_2O_2 + 0.67 mM $HgCl_2$	177.9	11.2	0.91	11.4
PBS + 0.3 μM H_2O_2 + 0.80 mM $HgCl_2$	176.3	11.1	0.91	9.1

The accuracy of the obtained electrochemical parameters (Table 3) was verified using chi-square goodness-of-fit test (Equation (3)), which evaluates the closeness of the observed values (Equation (3), symbol "*Oi*") to those obtained by the fitted model (Equation (3), symbol "*Ei*") [50,51]:

$$\chi^2 = \sum \frac{(O_i - E_i)^2}{E_i} \quad (3)$$

The subscript "*i*" in Equation (3) represents each element of the equivalent circuit; the function "χ^2" is known as "Chi Square Goodness of Fit Coefficient". The best fit is observed when the value of "χ^2" approaches zero.

It was found that the values of the equivalent circuit elements (Table 3) fitted appropriately to the experimental data (χ^2 varied from 1×10^{-5} to 5×10^{-4}). Even though the addition of H_2O_2 into the PBS did not cause a significant visual change in the EIS spectra (Figure 5), the value of the charge transfer resistance (R_{ct}) decreased from 960 to 576 kΩ cm^2 after adding H_2O_2 into the PBS (Table 3), indicating that some molecules of H_2O_2 were able to penetrate through the catalase layer and be reduced on the PB. This finding corresponds to the chronoamperometric investigation of the glass | FTO | PB | Cat electrode (Figure 3A), revealing that the addition of H_2O_2 to PBS causes a negligible reduction current (−0.7 μA cm^{-2}).

As predicted from the shape of the FFT-EIS spectra (Figure 5), the value of the charge transfer resistance (R_{ct}) decreases with an increasing concentration of Hg^{2+} ions. Furthermore, a linear dependence (R^2 = 0.994) of the Hg^{2+} ions-caused decrement in ΔR_{ct} on the concentration of Hg^{2+} ions (c^{-1} (Hg^{2+})) was observed in the range of 0.13 mM to 0.80 mM, with a sensitivity of 11.0 kΩ mM^{-1} (Figure 6). ΔR_{ct} was calculated by subtracting the R_{ct} values measured in the Hg^{2+}- and H_2O_2-containing PBS from the R_{ct} value (576 kΩ cm^2) measured in the H_2O_2-containing PBS (Table 3). Although this linear range (from 0.13 mM to 0.80 mM) is smaller than the linear range obtained during the amperometric study of the glass | FTO | PB electrode (Figure 3B, from 0.07 mM to 3 mM), the FFT-EIS method seems to be very promising for the detection of Hg^{2+} ions because of its ability to obtain a single spectrum very quickly—within 1 s. In addition, compared to other electrochemical techniques (e.g., fixed potential chronoamperometry), electrochemical impedance spectroscopy has several useful features, including the ability to perform a non-destructive measurement and the ability to distinguish the electrochemical parameter of interest (in this paper the charge transfer resistance) from other processes (e.g., diffusion) that affect the electrochemical signal [52,53]. In summary, the impedimetric detection of Hg^{2+} ions is significantly faster than the amperometric technique, which requires approximately 20 min to detect the Hg^{2+}-induced increase in the cathodic current (Figure 3).

The glass | FTO | PB | Cat electrode, as well as other enzyme inhibition-based biosensors, may be affected by the presence of other catalase-inhibiting compounds in the sample being analyzed. Previous studies [54–56] have shown that some pesticides and the ions of other heavy metals (e.g., Zn, Pb, Cd, Cu and Cr) can also reduce the activity of catalase. However, a previous study [54] indicated that Hg^{2+} ions inhibited catalase 1.5 to 3 times more efficiently than some other heavy metal ions (e.g., Zn, Cr, Cd and Pb) when the concentration of these ions varied from 10 mg mL^{-1} to 40 mg mL^{-1}. Therefore, the glass | FTO | PB | Cat

biosensor should be more sensitive to Hg^{2+} than to Zn, Cr, Cd or Pb ions. However, to ensure the high reliability of Hg^{2+} ion analysis with the glass | FTO | PB | Cat biosensor, a qualitative analysis of other heavy metal ions should also be performed.

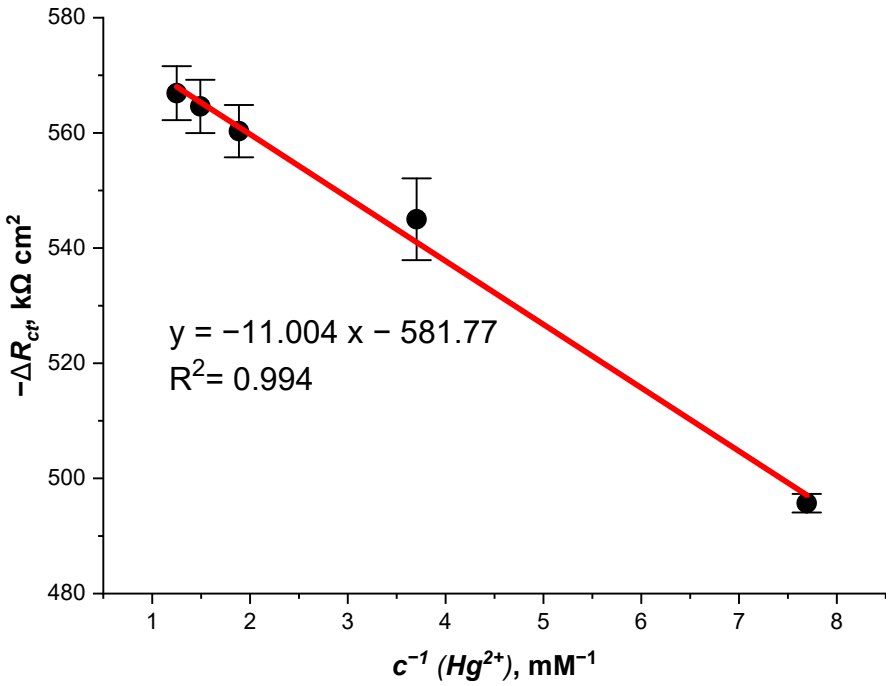

Figure 6. Dependence of the Hg^{2+} ions-caused decrement in the charge transfer resistance (ΔR_{ct}) on the concentration of Hg^{2+} ions (c^{-1} (Hg^{2+})).

4. Conclusions

In this study it was demonstrated that the glass | FTO | PB | Cat-based biosensor can be used to measure Hg^{2+} ions concentration in a buffer solution and in tap water. An application of PB in the composition of the Hg^{2+} ion biosensor enabled the use of a comparatively low potential of +0.2 V for the operation of the biosensor, reducing the probability of interfering oxidation reactions from other electrochemically-active substances which might be present in the analyzed sample (e.g., alkylphenols and sulfite ions) [44,45]. Furthermore, the Hg^{2+} ion biosensor constructed in this study showed that the chronoamperometric response decreased only about 10% during the first 2 weeks. This indicates a sufficient stability of the biosensor over time.

Chronoamperometry and FFT-EIS studies of the glass | FTO | PB | Cat-based biosensor in a Hg^{2+} ion-containing PBS enabled linear ranges of 0.07 mM–3 mM and 0.13 mM–0.80 mM of Hg^{2+} ions with a sensitivity of 15 μA cm^{-2} mM^{-1} and 11.3 kΩ mM^{-1}, respectively. In addition, the FFT-EIS technique allowed a very fast (within 1 s) measurement of the Hg^{2+} ion concentration. Considering that the Hg^{2+} ion biosensor developed in this study does not require expensive materials (e.g., metal nanoparticles) for its preparation, has a simple structure and is suitable for performing a very rapid analysis of Hg^{2+} ions, the glass | FTO | PB | Cat electrode-basedHg^{2+} ion biosensor seems to be a promising technique for determining the Hg^{2+} ion concentration in environmental samples, e.g., water or extracts from soil and sediments.

Author Contributions: Conceptualization, P.V. and A.V.; methodology, P.V. and N.D.; validation, P.V., N.D. and A.V.; formal analysis, P.V.; investigation, N.D.; resources, A.V.; data curation, A.V.; writing—original draft preparation, N.D., P.V. and A.V.; writing—review and editing, P.V. and A.V.; visualization, N.D.; supervision, A.V. All authors have read and agreed to the published version of the manuscript.

Funding: This research received no external funding.

Institutional Review Board Statement: Not applicable.

Informed Consent Statement: Not applicable.

Data Availability Statement: The data presented in this study are available on request from the corresponding author.

Conflicts of Interest: The authors declare there are no conflict of interest.

References

1. Bernhoft, R.A. Mercury Toxicity and Treatment: A Review of the Literature. *J. Environ. Public Health* **2012**, *2012*, 460508. [CrossRef]
2. Berlin, M.; Jerksell, L.G.; von Ubisch, H. Uptake and Retention of Mercury in the Mouse Brain. *Arch. Environ. Health Int. J.* **1966**, *12*, 33–42. [CrossRef] [PubMed]
3. Berlin, M.; Fazackerley, J.; Nordberg, G.; Kand, M. The Uptake of Mercury in the Brains of Mammals Exposed to Mercury Vapor and to Mercuric Salts. *Arch. Environ. Health Int. J.* **1969**, *18*, 719–729. [CrossRef] [PubMed]
4. Kosta, L.; Byrne, A.R.; Zelenko, V. Correlation between selenium and mercury in man following exposure to inorganic mercury. *Nature* **1975**, *254*, 238–239. [CrossRef] [PubMed]
5. Pendergrass, J.C.; Haley, B.E.; Vimy, M.J.; Winfield, S.A.; Lorscheider, F.L. Mercury vapor inhalation inhibits binding of GTP to tubulin in rat brain: Similarity to a molecular lesion in Alzheimer diseased brain. *Neurotoxicology* **1997**, *18*, 315–324.
6. Clifton, J.C. Mercury Exposure and Public Health. *Pediatr. Clin. N. Am.* **2007**, *54*, 237.e1–237.e45. [CrossRef]
7. Tinkov, A.A.; Ajsuvakova, O.; Skalnaya, M.; Popova, E.; Sinitskii, A.; Nemereshina, O.; Gatiatulina, E.; Nikonorov, A.; Skalny, A.V. Mercury and metabolic syndrome: A review of experimental and clinical observations. *Biometals* **2015**, *28*, 231–254. [CrossRef]
8. Chen, L.; Zhang, J.; Zhu, Y.; Zhang, Y. Molecular interaction of inorganic mercury(ii) with catalase: A spectroscopic study in combination with molecular docking. *RSC Adv.* **2015**, *5*, 79874–79881. [CrossRef]
9. Maghsoudi, A.S.; Hassani, S.; Mirnia, K.; Abdollahi, M. Recent Advances in Nanotechnology-Based Biosensors Development for Detection of Arsenic, Lead, Mercury, and Cadmium. *Int. J. Nanomed.* **2021**, *16*, 803–832. [CrossRef]
10. Gworek, B.; Dmuchowski, W.; Baczewska-Dąbrowska, A.H. Mercury in the terrestrial environment: A review. *Environ. Sci. Eur.* **2020**, *32*, 128. [CrossRef]
11. Gray, J.E.; Theodorakos, P.M.; Fey, D.L.; Krabbenhoft, D.P. Mercury concentrations and distribution in soil, water, mine waste leachates, and air in and around mercury mines in the Big Bend region, Texas, USA. *Environ. Geochem. Health* **2015**, *37*, 35–48. [CrossRef] [PubMed]
12. Bernaus, A.; Gaona, X.; van Ree, D.; Valiente, M. Determination of mercury in polluted soils surrounding a chlor-alkali plant: Direct speciation by X-ray absorption spectroscopy techniques and preliminary geochemical characterisation of the area. *Anal. Chim. Acta* **2006**, *565*, 73–80. [CrossRef]
13. Hylander, L.D.; Meili, M. 500 years of mercury production: Global annual inventory by region until 2000 and associated emissions. *Sci. Total Environ.* **2003**, *304*, 13–27. [CrossRef] [PubMed]
14. Higueras, P.; Oyarzun, R.; Biester, H.; Lillo, J.; Lorenzo, S. A first insight into mercury distribution and speciation in soils from the Almadén mining district, Spain. *J. Geochem. Explor.* **2003**, *80*, 95–104. [CrossRef]
15. Ullrich, S.M.; Ilyushchenko, M.A.; Kamberov, I.M.; Tanton, T.W. Mercury contamination in the vicinity of a derelict chlor-alkali plant. Part I: Sediment and water contamination of Lake Balkyldak and the River Irtysh. *Sci. Total Environ.* **2007**, *381*, 1–16. [CrossRef]
16. Geng, W.; Nakajima, T.; Takanashi, H.; Ohki, A. Determination of mercury in ash and soil samples by oxygen flask combustion method–Cold vapor atomic fluorescence spectrometry (CVAFS). *J. Hazard. Mater.* **2008**, *154*, 325–330. [CrossRef]
17. Pourreza, N.; Ghanemi, K. Determination of mercury in water and fish samples by cold vapor atomic absorption spectrometry after solid phase extraction on agar modified with 2-mercaptobenzimidazole. *J. Hazard. Mater.* **2009**, *161*, 982–987. [CrossRef]
18. Voegborlo, R.; Akagi, H. Determination of mercury in fish by cold vapour atomic absorption spectrometry using an automatic mercury analyzer. *Food Chem.* **2007**, *100*, 853–858. [CrossRef]
19. Fernández, Z.H.; Rojas, L.A.V.; Álvarez, A.M.; Álvarez, J.R.E.; dos Santos, J.A.; González, I.P.; González, M.R.; Macias, N.A.; Sánchez, D.L.; Torres, D.H. Application of Cold Vapor-Atomic Absorption (CVAAS) Spectrophotometry and Inductively Coupled Plasma-Atomic Emission Spectrometry methods for cadmium, mercury and lead analyses of fish samples. Validation of the method of CVAAS. *Food Control* **2015**, *48*, 37–42. [CrossRef]
20. Zheng, C.; Li, Y.; He, Y.; Ma, Q.; Hou, X. Photo-induced chemical vapor generation with formic acid for ultrasensitive atomic fluorescence spectrometric determination of mercury: Potential application to mercury speciation in water. *J. Anal. At. Spectrom.* **2005**, *20*, 746–750. [CrossRef]
21. Allibone, J.; Fatemian, E.; Walker, P.J. Determination of mercury in potable water by ICP-MS using gold as a stabilising agent. *J. Anal. At. Spectrom.* **1999**, *14*, 235–239. [CrossRef]
22. Baxter, D.C.; Frech, W. Determination of mercury by atomic absorption spectrometry using a platinum-lined graphite furnace for in situ preconcentration. *Anal. Chim. Acta* **1989**, *225*, 175–183. [CrossRef]
23. Okamoto, Y.; Kumamaru, T.; Hara, S.; Matsuo, H.; Kiboku, M. Determination of Mercury by Graphite Furnace Atomic Absorption Spectrometry after Ion-Pair Extraction with Zephiramine in Small Scale. *Bull. Chem. Soc. Jpn.* **1987**, *60*, 3053–3055. [CrossRef]

24. Zeiner, M.; Rezić, I.; Steffan, I. Analytical Methods for the Determination of Heavy Metals in the Textile Industry, Kemija u Industriji. *Časopis Kemičara Kem. Inženjera Hrvat.* **2007**, *56*, 587–595.
25. Nuttall, K.L.; Gordon, W.H.; Ash, K.O. Inductively coupled plasma mass spectrometry for trace element analysis in the clinical laboratory. *Ann. Clin. Lab. Sci.* **1995**, *25*, 264–271.
26. Malhotra, B.D.; Ali, A. *Nanomaterials in Biosensors: Fundamentals and Applications*; Elsevier: Amsterdam, The Netherlands, 2018; pp. 1–74. [CrossRef]
27. Domínguez-Renedo, O.; Alonso-Lomillo, M.; Ferreira-Gonçalves, L.; Arcos-Martínez, M. Development of urease based amperometric biosensors for the inhibitive determination of Hg (II). *Talanta* **2009**, *79*, 1306–1310. [CrossRef]
28. Ayenimo, J.G.; Adeloju, S.B. Rapid amperometric detection of trace metals by inhibition of an ultrathin polypyrrole-based glucose biosensor. *Talanta* **2016**, *148*, 502–510. [CrossRef]
29. Zhang, Y.; Zhang, C.; Ma, R.; Du, X.; Dong, W.; Chen, Y.; Chen, Q. An ultra-sensitive Au nanoparticles functionalized DNA biosensor for electrochemical sensing of mercury ions. *Mater. Sci. Eng. C* **2017**, *75*, 175–181. [CrossRef]
30. Elsebai, B.; Ghica, M.E.; Abbas, M.N.; Brett, C.M. Catalase based hydrogen peroxide biosensor for mercury determination by inhibition measurements. *J. Hazard. Mater.* **2017**, *340*, 344–350. [CrossRef]
31. Guascito, M.R.; Malitesta, C.; Mazzotta, E.; Turco, A. Inhibitive determination of metal ions by an amperometric glucose oxidase biosensor: Study of the effect of hydrogen peroxide decomposition. *Sens. Actuators B Chem.* **2008**, *131*, 394–402. [CrossRef]
32. Kuralay, F.; Özyörük, H.; Yıldız, A. Inhibitive determination of Hg2+ ion by an amperometric urea biosensor using poly(vinylferrocenium) film. *Enzym. Microb. Technol.* **2007**, *40*, 1156–1159. [CrossRef]
33. Mohammadi, H.; Amine, A.; Cosnier, S.; Mousty, C. Mercury–enzyme inhibition assays with an amperometric sucrose biosensor based on a trienzymatic-clay matrix. *Anal. Chim. Acta* **2005**, *543*, 143–149. [CrossRef]
34. Tan, I.; Erhan, E.; Karagöz, P.; Özkan, M. Determination of mercury and nickel by amperometric biosensor prepared with thermostable lactate dehydrogenase. *Trans. Nonferrous Met. Soc. China* **2011**, *21*, 2332–2338. [CrossRef]
35. Liu, J.-X.; Xu, X.-M.; Tang, L.; Zeng, G.-M. Determination of trace mercury in compost extract by inhibition based glucose oxidase biosensor. *Trans. Nonferrous Met. Soc. China* **2009**, *19*, 235–240. [CrossRef]
36. Popkirov, G.S.; Schindler, R.N. A new impedance spectrometer for the investigation of electrochemical systems. *Rev. Sci. Instrum.* **1992**, *63*, 5366–5372. [CrossRef]
37. Gabriunaite, I.; Valiūnienė, A.; Valincius, G. Formation and properties of phospholipid bilayers on fluorine doped tin oxide electrodes. *Electrochim. Acta* **2018**, *283*, 1351–1358. [CrossRef]
38. Valiūnienė, A.; Kavaliauskaitė, G.; Virbickas, P.; Ramanavičius, A. Prussian blue based impedimetric urea biosensor. *J. Electroanal. Chem.* **2021**, *895*, 115473. [CrossRef]
39. Valiūnienė, A.; Virbickas, P.; Medvikytė, G.; Ramanavičius, A. Urea Biosensor Based on Electrochromic Properties of Prussian Blue. *Electroanalysis* **2020**, *32*, 503–509. [CrossRef]
40. Noël, J.-M.; Médard, J.; Combellas, C.; Kanoufi, F. Prussian Blue Degradation during Hydrogen Peroxide Reduction: A Scanning Electrochemical Microscopy Study on the Role of the Hydroxide Ion and Hydroxyl Radical. *Chemelectrochem* **2016**, *3*, 1178–1184. [CrossRef]
41. Alfonso-Prieto, M.; Biarnés, X.; Vidossich, P.; Rovira, C. The Molecular Mechanism of the Catalase Reaction. *J. Am. Chem. Soc.* **2009**, *131*, 11751–11761. [CrossRef]
42. Hermes, M.; Scholz, F. The electrochemical determination of ammonium based on the selective inhibition of the low-spin iron(II)/(III) system of Prussian blue. *J. Solid State Electrochem.* **1997**, *1*, 215–220. [CrossRef]
43. Virbickas, P.; Valiūnienė, A.; Kavaliauskaitė, G.; Ramanavicius, A. Prussian White-Based Optical Glucose Biosensor. *J. Electro-Chem. Soc.* **2019**, *166*, B927–B932. [CrossRef]
44. Chmayssem, A.; Hauchard, D. New Detection Method for Alkylphenol Traces in Water Based on an Integrated Electrochemical Cell Sensor. *J. Water Sci.* **2015**, *28*, 35–40. [CrossRef]
45. Novgorodtseva, O.N.; Zelinsky, A. Effects of solution pH on sulfite oxidation at a gold electrode. *J. Solid State Electrochem.* **2019**, *23*, 2301–2306. [CrossRef]
46. Ayenimo, J.G.; Adeloju, S.B. Inhibitive potentiometric detection of trace metals with ultrathin polypyrrole glucose oxidase biosensor. *Talanta* **2015**, *137*, 62–70. [CrossRef] [PubMed]
47. Yu, J.; Guan, H.; Chi, D. An amperometric glucose oxidase biosensor based on liposome microreactor-chitosan nanocompo-site-modified electrode for determination of trace mercury. *J. Solid State Electrochem.* **2017**, *21*, 1175–1183. [CrossRef]
48. Virbickas, P.; Ziziunaite, G.; Ramanavicius, A.; Valiūnienė, A. Prussian Blue Modified Amperometric Hg^{2+} Ion Biosensor Based on Glucose Oxidase Inhibition. *Electroanalysis* **2022**, *35*, e202200230. [CrossRef]
49. Ashrafi, A.M.; Sýs, M.; Sedláčková, E.; Farag, A.S.; Adam, V.; Přibyl, J.; Richtera, L. Application of the Enzymatic Electrochemical Biosensors for Monitoring Non-Competitive Inhibition of Enzyme Activity by Heavy Metals. *Sensors* **2019**, *19*, 2939. [CrossRef]
50. Website of the Department of Statistics and Data Science of Yale University. Chi-Square Goodness of Fit Test. Available online: http://www.stat.yale.edu/Courses/1997-98/101/chigf.htm (accessed on 27 April 2023).
51. Virbickas, P.; Valiūnienė, A.; Baryševa, D.; Popkirov, G.; Ramanavičius, A. Determination of cyanide concentration by chronoamperometry, cyclic voltammetry and fast Fourier transform electrochemical impedance spectroscopy. *J. Electroanal. Chem.* **2021**, *895*, 115449. [CrossRef]

52. Magar, H.S.; Hassan, R.Y.A.; Mulchandani, A. Electrochemical Impedance Spectroscopy (EIS): Principles, Construction, and Biosensing Applications. *Sensors* **2021**, *21*, 6578. [CrossRef]
53. Li, S.; Zhou, Q.; Cong, H. Electrochemical Techniques, Impedance, and Spectroscopy. In *Handbook of Advanced Non-Destructive Evaluation*; Springer: Berlin/Heidelberg, Germany, 2018; pp. 1–27. [CrossRef]
54. Singh, S.M.; Sivalingam, P.M. In vitro study on the interactive effects of heavy metals on catalase activity of Sarotherodon mossambicus (Peters). *J. Fish Biol.* **1982**, *20*, 683–688. [CrossRef]
55. Yeboah, J.O.; Shi, G.; Shi, W. Effect of Heavy Metal Contamination on Soil Enzymes Activities. *J. Geosci. Environ. Prot.* **2021**, *9*, 135–154. [CrossRef]
56. Karadag, H.; Ozhan, F. Effect of cyprodinil and fludioxonil pesticides on bovine liver catalase activity. *Biotechnol. Biotechnol. Equip.* **2015**, *29*, 40–44. [CrossRef] [PubMed]